

# Effect of micro-CT acquisition parameters and individual analysis on the assessment of bone repair

Milena Suemi IRIE<sup>(a)</sup>   
Rubens SPIN-NETO<sup>(b)</sup>   
Lucas Henrique Souza TEIXEIRA<sup>(a)</sup>   
Gustavo Davi RABELO<sup>(c)</sup>   
Nayara Teixeira de Araújo REIS<sup>(a)</sup>   
Priscilla Barbosa Ferreira SOARES<sup>(a)</sup> 

<sup>(a)</sup>Universidade Federal de Uberlândia – UFU, School of Dentistry, Department of Periodontology and Implantology, Uberlândia, MG, Brazil.

<sup>(b)</sup>Aarhus University, Department of Dentistry and Oral Health, Health, Aarhus, Denmark.

<sup>(c)</sup>Universidade Federal de Santa Catarina, Dentistry Department, Florianópolis, SC, Brazil.

**Declaration of Interests:** The authors certify that they have no commercial or associative interest that represents a conflict of interest in connection with the manuscript.

## Corresponding Author:

Priscilla Barbosa Ferreira Soares  
E-mail: pbfsoares@yahoo.com.br

<https://doi.org/10.1590/1807-3107bor-2023.vol37.0099>

Submitted: September 27, 2021  
Accepted for publication: August 23, 2022  
Last revision: September 19, 2022

**Abstract:** This study aimed to investigate whether two acquisition parameters, voxel size and filter thickness, used in a micro-computed tomography (micro-CT) scan, together with the examiner's experience, influence the outcome of bone repair analysis in an experimental model. Bone defects were created in rat tibiae and scanned using two voxel sizes of 6- or 12- $\mu$ m and two aluminum filter thickness of 0.5- or 1-mm. Then, bone volume fraction (BV/TV) and trabecular thickness (Tb.Th) were analyzed twice by two groups of operators: experienced and inexperienced examiners. For BV/TV, no significant differences were found between scanning voxel sizes of 6 and 12  $\mu$ m for the experienced examiners; however, for the inexperienced examiners, the analysis performed using a 12- $\mu$ m voxel size resulted in higher BV/TV values (32.4 and 32.9) than those acquired using a 6- $\mu$ m voxel size (25.4 and 24.8) ( $p < 0.05$ ). For Tb.Th, no significant differences between the analyses performed by experienced and inexperienced groups were observed when using the 6- $\mu$ m voxel size. However, inexperienced examiners' analysis revealed higher Tb.Th values when using the 12- $\mu$ m voxel size compared with 6  $\mu$ m (0.05 *vs.* 0.03,  $p < 0.05$ ). Filter thickness had no influence on the results of any group. In conclusion, voxel size and operator experience affected the measured Tb.Th and BV/TV of a region with new bone formation. Operator experience in micro-CT analysis is more critical for BV/TV than for Tb.Th, whereas voxel size significantly affects Tb.Th evaluation. Operators in the initial phases of research training should be calibrated for bone assessments.

**Keywords:** X-Ray Microtomography; Bone and Bones; Wound Healing; Models, Animal; Cancellous Bone.

## Introduction

Microcomputed tomography (micro-CT) analysis is a nondestructive method that provides three-dimensional reconstruction of interior structures and other bone properties.<sup>1,2</sup> Several studies have reported a strong correlation between micro-CT and histomorphometric analysis.<sup>3,4</sup> Micro-CT is widely used in the fields of bone metabolism, repair, and regeneration.<sup>5</sup> The acquisition and analysis of bone volumes using micro-CT consists of the following steps: a) scout view and preprocessing of 2D section visualization, b) sample scanning, c) segmentation and 3D



reconstruction, and d) microstructure quantification and analysis. At each stage of this process, some variables, such as resolution and use of filters, may affect the morphological outcomes.<sup>6</sup> A guideline based on the need for standardized terminology and consistent reporting of parameters analyzed was published,<sup>1</sup> and it was described that in addition to manufacturer-specific instructions for regular quality control, images should be inspected visually to identify possible scanning artifacts. Thus, the influence of scanning and image processing during analysis and its influence on the results still need to be assessed.

Image resolution is determined by voxel size. Morphological assessment of thinner structures, such as rat bone trabeculae (20–70  $\mu\text{m}$ ), can be affected by resolution.<sup>3,7</sup> Scanning small structures with low resolution can underestimate bone mineral density and overestimate its thickness.<sup>8</sup> Most micro-CT systems provide a resolution on the order of 6–73  $\mu\text{m}$ .<sup>9</sup> Ideally, the smallest voxel size (highest resolution) should be used in animal experiments; however, using a small voxel size increases the scanning duration and data generation, sometimes becoming too time-consuming. Moreover, the amount of radiation must be considered when applying *in vivo* micro-CT scanning.<sup>6</sup>

Another acquisition parameter that influences the quality of results is the use of filters, which may minimize the artifacts present in the images. Beam hardening is an artifact produced by polychromatic X-ray beams with different energy spectra. When the X-ray beam propagates through the sample, the low-energy portion stops in the surface area, whereas the high-energy portion remains inside the sample. This phenomenon manifests as a high-density image of the surface of the sample. This artifact can be minimized during the reconstruction stage. However, by placing a metal filter between the X-ray and the sample during image acquisition, the lower energy portion of the beam is filtered. The ideal filter and filter thickness to use will also depend on sample size and density.<sup>1</sup>

The region of interest (ROI; *e.g.*, the specific site where bone healing will be assessed in this study) should be delimited and separated from the other

structures across the acquired field of view.<sup>5,10–12</sup> This process can be performed either manually or automatically. After ROI delimitation, determining a grayscale threshold (0–255) distinguishes bone from non-bone, a process called image segmentation (or binarization). This process can be performed using local or global values. Most commonly, global thresholding is performed, in which a chosen value (Hounsfield units or  $\text{g}/\text{cm}^3$ ) distinguishes bone (above the threshold) from non-bone (below the threshold). The threshold is selected either visually by analyzing the density of the histogram or by setting a threshold value that will result in a volume dataset equal to the volume of the original bone sample.<sup>13</sup> Local thresholds are based on the neighboring values of each voxel<sup>14</sup> or on the local minima and local maxima values of the selected ROI. Diverse methods applying the local threshold definition have been reported<sup>15,16</sup> to overcome the limitations related to low-resolution and nonhomogeneous samples that affect global thresholding. However, both processes (ROI delimitation and threshold setting) are influenced by the examiner's experience.

This study aimed to investigate whether the acquisition voxel size, filter thickness, and operator experience affect the morphometric outcome of bone repair evaluation assessed using micro-CT. The null hypothesis was that the acquisition voxel size, filter thickness, and examiner experience have no effect on the outcome.

## Methodology

This study was approved by the Research Ethics Committee (approval number 093/17) of the institution and was carried out in strict compliance with the ethical principles for the care and use of laboratory animals in accordance with the ARRIVE guidelines. Cortical bone defects (1.6 mm diameter) were created using a cylindrical burr (Neodent®, Curitiba, Brazil) at a standardized location on the tibiae of five Wistar rats. The animals were euthanized 7 days after surgery, and the right tibiae were covered with moist gauze containing phosphate-buffered solution and stored in plastic tubes at  $-20^\circ\text{C}$  until scanning. The tibiae were positioned in

the sample holder and left at room temperature before scanning. Micro-CT scans of the five tibiae (Figure 1) were acquired with a desktop SkyScan 1272 high-resolution 3D X-ray microscope based on micro-CT technology (Bruker, Kontich, Belgium).

Each sample was repeatedly scanned using the following acquisition parameters: voxel sizes of 6  $\mu\text{m}$  and 12  $\mu\text{m}$ , as well as aluminum filter thicknesses of 0.5 mm and 1.0 mm ( $n = 5$ ). Image reconstruction was performed using NRecon software (version 1.6.6.0, Bruker, Kontich, Belgium). A single set of parameters was chosen visually based on the minimum artifacts, irrespective of the test group. The ring artifact correction was set at 9, smoothing at 1, and beam-hardening correction at 0%. The reconstructions included the entire lesion as follows: new bone formation inside the tibial canal and at the lesion site was manually delimited in 2D slices (Figure 2), from the bottom to the top of the lesion borders, delineated by a single examiner (LHST).

Morphometric data (bone volume ratio, BV/TV; trabecular thickness in  $\mu\text{m}$ , Tb.Th) were evaluated by five experienced and five inexperienced examiners and assessed for each acquisition parameter. The inexperienced examiner's group included operators with experience in micro-CT analysis, but none had ever performed bone analysis before the study. The experienced examiner's group included researchers who had performed micro-CT analysis of rat bone tissue in previous experiments and other bone analyses. BV/TV and Tb.Th analyses were performed using the CTA software (version 1.18.4.0, Bruker,

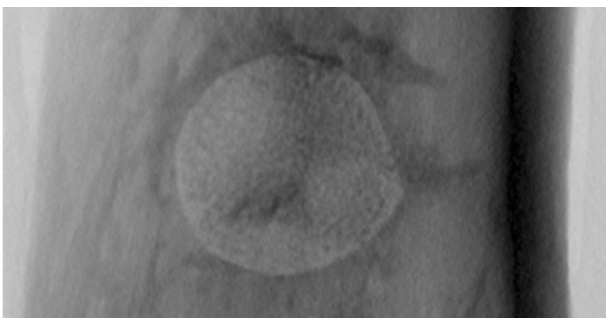


**Figure 1.** Micro-CT scout view of the tibia with the cortical defect (6  $\mu\text{m}$  voxel size at 70 kV, 142  $\mu\text{A}$ , a 0.2 rotation step, and a 1 mm aluminum filter).

Kontich, Belgium). Trabecular bone segmentation within the lesion area was manually performed by each examiner. The entire lesion was defined by interpolation of the ROIs delineated by each examiner. The thresholds for the segmentation of bone and non-bone (maximum and minimum gray levels) were visually and individually defined for each set of acquisition parameters. The BV/TV and Tb.Th values were then calculated.

Statistical analysis was performed using SigmaPlot® (SigmaPlot v13.1; Systat Software Inc., Systat Software Inc., San Jose, USA), with a significance level of  $\alpha = 0.05$ . The influence of operator experience (experienced and inexperienced examiners), filter thickness (aluminum 0.5 and 1 mm), and scanning voxel size (6 and 12  $\mu\text{m}$ ) on BV/TV and Tb.Th were assessed using three-way analysis of variance (ANOVA) with Tukey's post hoc test. Intraclass correlation coefficients (ICCs) for absolute agreement among total tissue volume measurements were calculated<sup>17</sup> (MATLAB MathWorks, Natick, USA) to evaluate inter-examiner reliability<sup>16</sup> for cortical and trabecular bone segmentation in both the experienced and inexperienced groups.

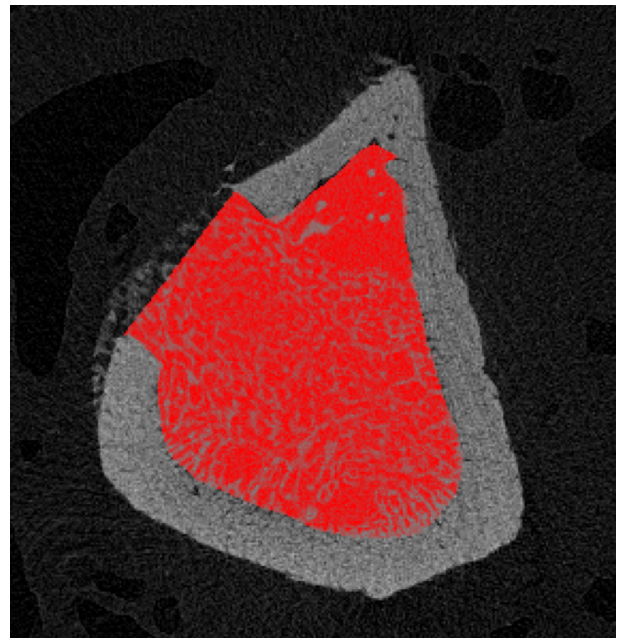


**Figure 2.** Demonstration of the region of interest (ROI) delimitation of the defect area.

## Results

The ICC between experienced examiners was 0.84, indicating good reliability. Thus, the ICC between the inexperienced examiners indicated poor reliability (0.06). The mean and standard deviation values for BV/TV and Tb.Th are summarized in Tables 1 and 2, respectively. The factor interactions (operator experience, voxel size, and filter) for BV/TV and Tb.Th are presented in Tables 3 and 4, respectively.

### BV/TV

Operator experience ( $p < 0.001$ ), voxel size ( $p < 0.001$ ), and the interaction between these factors ( $p = 0.009$ ) had significant effects on BV/TV (Table 3). The analysis performed by experienced examiners

resulted in significantly lower BV/TV values than those performed by inexperienced examiners (Table 1). The effect of voxel size depends on the examiner's experience. No significant difference was observed for the experienced examiners after scanning at voxel sizes of 6 ( $15.5 \pm 4.0$  and  $16 \pm 5$ ; for 0.5 and 1 mm filter, respectively) and 12  $\mu\text{m}$  ( $16.1 \pm 5.1$  and  $15.1 \pm 4.9$ ; for 0.5 and 1 mm filter, respectively) ( $p = 0.900$ ). However, for the inexperienced examiners, the analysis performed on the 12  $\mu\text{m}$  volumes resulted in higher BV/TV ( $32.4 \pm 15.1$  and  $32.9 \pm 16.1$ ; for 0.5 and 1 mm filter, respectively) than that performed on the 6  $\mu\text{m}$  group ( $25.4 \pm 14.1$  and  $24.8 \pm 14.5$ ; for the 0.5 and 1 mm filter, respectively). The effects of the filter and its interactions with the tested factors were insignificant. No significant interaction was found between the three factors ( $p = 0.500$ ).

**Table 1.** Mean BV/TV values (SDs) and results of Tukey HSD test.

Examiner	6 $\mu\text{m}$ voxel size		12 $\mu\text{m}$ voxel size	
	0.5mm filter	1.0mm filter	0.5mm filter	1.0mm filter
Experienced	15.5 (4.0) <sup>Aa</sup>	16.0 (5.0) <sup>Aa</sup>	16.1 (5.6) <sup>Aa</sup>	15.1 (4.9) <sup>Aa</sup>
Non-experienced	25.4 (14.1) <sup>Ba</sup>	24.8 (14.5) <sup>Ba</sup>	32.4 (15.1) <sup>Bb</sup>	32.9 (16.1) <sup>Bb</sup>

Different uppercase letters in vertical columns indicate significant differences; different lowercase letters in horizontal rows indicate significant differences; Tukey HSD test ( $p < 0.05$ ).

**Table 2.** Mean Tb.Th values (SDs) and results of Tukey HSD test.

Examiner	6 $\mu\text{m}$ voxel size		12 $\mu\text{m}$ voxel size	
	0.5mm filter	1.0mm filter	0.5mm filter	1.0mm filter
Experienced	0.04 (0.01) <sup>Aa</sup>	0.03 (0.01) <sup>Aa</sup>	0.06 (0.02) <sup>Ab</sup>	0.06 (0.02) <sup>Ab</sup>
Non-experienced	0.03 (0.00) <sup>Aa</sup>	0.03 (0.00) <sup>Aa</sup>	0.05 (0.01) <sup>Bb</sup>	0.05 (0.00) <sup>Bb</sup>

Different uppercase letters in vertical columns indicate significant differences; different lowercase letters in horizontal rows indicate significant differences; Tukey HSD test ( $p < 0.05$ ).

**Table 3.** Three-way ANOVA interactions for BV/TV measurements.

Source of variation	p-values
Operators x Filter	0.800
Operators x Voxel size	0.009*
Filter x Voxel size	0.800
Operators x Filter x Voxel size	0.500

\*The mean difference is significant at the 0.05 level.

**Table 4.** Three-way ANOVA interactions for Tb.Th measurements.

Source of variation	p-values
Operators x Filter	0.400
Operators x Voxel size	0.040*
Filter x Voxel size	0.400
Operators x Filter x Voxel size	0.900

\*The mean difference is significant at the 0.05 level.

## Tb.Th

The examiner ( $p < 0.001$ ), voxel size ( $p < 0.001$ ), and interaction between factors ( $p = 0.040$ ) had significant effects on Tb.Th (Table 4). The analysis performed by experienced examiners resulted in lower Tb.Th values than those performed by inexperienced examiners ( $p < 0.001$ ). The examiner depended on the voxel size of the analyzed volumes. There was no difference between the experienced and inexperienced operators in the 6  $\mu\text{m}$  group ( $p = 0.900$ ); however, the analysis performed on 12  $\mu\text{m}$  volumes resulted in higher ( $p < 0.001$ ) Tb.Th values for the experienced examiners ( $0.06 \pm 0.02$  for both filters) than for the non-experienced examiners ( $0.05 \pm 0.01$  and  $0.05 \pm 0.0$ ; for 0.5 and 1 mm filter, respectively). The filter and interactions between two or three factors had no significant influence on the Tb.Th values ( $p = 0.900$ ).

## Discussion

The present study investigated whether the acquisition voxel size, filter thickness, and operator experience influenced the results of the morphometric evaluation of bone volume and trabecular thickness, using an experimental model of bone repair in rat tibiae. Both morphometric parameters of BV/TV and Tb.Th demonstrated some dependency on examiner experience and voxel size acquisition. The filter thickness also had no effect on the BV/TV and Tb.Th measurements. Thus, the null hypothesis that the acquisition voxel size, filter thickness, and experience of the examiner parameters have no effect on the outcome of the morphometric evaluation was partially rejected. Thus, the present study identified two critical factors that should be considered for micro-CT analysis of a site with new bone formation: acquisition voxel size and examiner experience.

Several segmentation methods have been described to separate trabeculae from the cortical bone in micro-CT volumes.<sup>10,17,18</sup> Automated segmentation to distinguish cortical from trabecular bone is not possible for bone repair sites in some specific models (mostly on the diaphysis of long bones) once the cortical contour is not intact and a detailed delimitation of the lesion edges cannot be achieved. If an ROI (e.g.,

a standardized circle) is defined in the cancellous region, the analysis can be underestimated when only a fraction of the ROI (i.e., trabecular bone undergoing healing) is included.<sup>10</sup> An automated method to identify and separate the callus and/or newly formed bone, original cortical bone, and marrow portion without requiring the delimitation of specific ROIs has been proposed previously.<sup>19</sup> The authors applied global thresholding to each structure visually determined by two independent examiners and by the associated histogram. This method was not time-consuming; however, it did not provide volume-dependent micro-CT assessments of parameters such as BV/TV. In this case, the most accurate method for non-intact cortical analysis is the manual drawing of contour lines on the outer edge of the lesion. Therefore, creating a volume of interest (VOI) by interpolating several ROIs is feasible considering the rupture in the cortical bone, the dimensions of which diverge in each section.

The ICC for the total volume indicated good reliability between the VOIs of experienced examiners. However, such good reliability was not observed among inexperienced examiners. This finding supports the difference in BV/TV outcomes between the groups. The bone volume fraction is one of the main morphological parameters for evaluating bone repair, and it depends on the total volume.<sup>1</sup> The results of the present study demonstrated that detailed VOI delimitation by an experienced and calibrated examiner is critical for bone volume fraction analysis of a healing area. The relevance of examiner experience is also emphasized over the effect of resolution. BV/TV was influenced by the acquisition voxel size only for inexperienced examiners. The analysis performed by an experienced examiner showed no difference between the voxel sizes of 6 and 12  $\mu\text{m}$ .

The influence of operator experience was also observed in Tb.Th measurements. However, this difference was only observed in the 12  $\mu\text{m}$  group, indicating that Tb.Th analysis of bone repair in rats is less biased when using 6  $\mu\text{m}$  voxel size volumes than with respect to the examiner. When acquiring volumes at a larger voxel size, the bone surface is blurred, especially for trabecular structures within

a healing area (which have higher resorption rates and thinner trabeculae).<sup>20</sup> This approach makes the binarization process more prone to bias, which is evident when the examiners have no previous experience in bone morphometric analysis. Longo et al.<sup>8</sup> compared 9  $\mu\text{m}$  and 18  $\mu\text{m}$  voxel sizes in both *in vivo* and *ex vivo* micro-CT. The authors demonstrated that analysis with smaller voxel volumes led to lower Tb.Th measurements in rat trabeculae. Similar results were found in the present study, in which a significant difference was observed between the 6- and 12- $\mu\text{m}$  groups for Tb.Th. The findings of the present study support the hypothesis that thinner trabecular structures are blurry when scanning at a larger voxel size, culminating in an increase in the mean measured thickness.

The effect of acquisition voxel size on trabecular structures has also been demonstrated in human cadaver investigations.<sup>21</sup> While the effect of acquisition voxel size has been observed at larger dimensions, such as 41  $\mu\text{m}$  in micro-CT compared to high-resolution peripheral quantitative computed tomography (HQ-pQCT) with acquisition voxel sizes of 41, 82, and 123  $\mu\text{m}$ , the results of the present study revealed the same effect, even for a narrow difference in voxel size during image acquisition. A smaller voxel size may allow a more accurate segmentation of the trabecular structure, which results in a more accurate quantification of the trabecular microstructure parameters. The acquisition resolution should always be chosen based on the size of the structure being analyzed as well as the size of the expected microarchitecture changes that the experimenter aims to quantify.<sup>22</sup> However, resolution might be critical if it involves remodeling of areas. Therefore, the present study has demonstrated that scanning at a 6  $\mu\text{m}$  or 12  $\mu\text{m}$  voxel size was not a limiting factor for BV/TV with calibrated examiners; rather, scanning at a 6  $\mu\text{m}$  voxel size is a determinant for Tb.Th measurements of a healing bone area.

In this study, a global threshold is used for each acquisition parameter. The cortical bone was removed from the analyzed area, and only the trabecular bone within the lesion was analyzed to provide a homogenous structure analysis. A local threshold method was proposed<sup>23</sup> and validated

using histological analysis. The authors concluded that the performance of global threshold methods is equal to that of local thresholds when analyzing high-resolution scans of homogenous structures. However, when nonhomogeneous samples are analyzed (*e.g.*, both thick cortices and thin trabeculae) or when the scan resolution is relatively low, the efficiency of the local threshold method exceeds that of global methods. When analyzing high-resolution volumes of a homogeneous bone sample, as in the present study, subjective thresholding performs similarly to objective thresholding. Nonetheless, a reliable threshold should be defined by considering 2D slice-wise comparisons to the original, regardless of the segmentation method. Visual inspection of the segmentations to ensure that trabecular connectivity is maintained, while excluding noise, is crucial for micro-CT analysis.<sup>21</sup> It was also reported that segmentation limitations could be mitigated by scanning at high-resolutions,<sup>22</sup> corrections for beam hardening, and implementation of a density-based thresholding method.

The effect of beam hardening can be reduced by placing a metal filter during scanning and applying corrective algorithms during the reconstruction.<sup>24</sup> In the present study, the beam-hardening correction was set at 0% to verify the effect of the filter without the algorithm correction. However, no difference was observed in either parameter (BV/TV or Tb.Th) between the 0.5- and 1-mm thick aluminum filters. It has been demonstrated that beam hardening leads to fewer morphological artifacts than densitometric measurements.<sup>25</sup> However, one of the limitations of the present study is that bone mineral density was not assessed to serve as a reference standard (*i.e.*, the truth); thus, we can only assume that aluminum filter thickness did not influence the morphometric outcomes. Despite this limitation, the importance of a single experienced examiner for all samples to avoid bias in morphometric outcomes was clear.

## Conclusions

Considering the limitations of the study design, it was possible to conclude the following:

- a. The acquisition voxel size (6 and 12  $\mu\text{m}$ ) and operator experience influenced the outcome of

the results obtained for trabecular thickness and bone volume ratio at the site of bone repair in an experimental model.

- b. The individual experience of the operator in micro-CT analysis is more critical for BV/TV, whereas voxel size has a major effect on Tb. Th.
- c. High-resolution acquisitions should be used whenever possible to provide the most accurate measurements of bone microstructure parameters in an area during an active repair process.

## Acknowledgements

The authors are grateful to the Rede de Biotérios de Roedores da UFU (REBIR-UFU), Centro de Pesquisa Odontológico - Biomecânica, Biomateriais e Biologia celular (CPBIO) and the others operators who collaborated on the analysis (Guilherme José Pimentel Lopes Oliveira, Pedro Henrique Justino Oliveira Limirio, Juliana Simeão Borges, Vitor Cardoso Costa, Victor Flores and Luis Gustavo Gonzales Osuna).

## References

1. Bouxsein ML, Boyd SK, Christiansen BA, Guldberg RE, Jepsen KJ, Müller R. Guidelines for assessment of bone microstructure in rodents using micro-computed tomography. *J Bone Miner Res.* 2010 Jul;25(7):1468-86. <https://doi.org/10.1002/jbmr.141>
2. Köhl S, Brochhausen C, Götz H, Filippi A, Payer M, d'Hoedt B, et al. The influence of bone substitute materials on the bone volume after maxillary sinus augmentation: a microcomputerized tomography study. *Clin Oral Investig.* 2013 Mar;17(2):543-51. <https://doi.org/10.1007/s00784-012-0732-2>
3. Müller R, Van Campenhout H, Van Damme B, Van Der Perre G, Dequeker J, Hildebrand T, et al. Morphometric analysis of human bone biopsies: a quantitative structural comparison of histological sections and micro-computed tomography. *Bone.* 1998 Jul;23(1):59-66. [https://doi.org/10.1016/S8756-3282\(98\)00068-4](https://doi.org/10.1016/S8756-3282(98)00068-4)
4. Anavi Y, Avishai G, Calderon S, Allon DM. Bone remodeling in onlay beta-tricalcium phosphate and coral grafts to rat calvaria: microcomputerized tomography analysis. *J Oral Implantol.* 2011 Aug;37(4):379-86. <https://doi.org/10.1563/AAID-JOI-D-09-00128.1>
5. Irie MS, Rabelo GD, Spin-Neto R, Dechichi P, Borges JS, Soares PB. Use of micro-computed tomography for bone evaluation in dentistry. *Braz Dent J.* 2018 May-Jun;29(3):227-38. <https://doi.org/10.1590/0103-6440201801979>
6. Christiansen BA. Effect of micro-computed tomography voxel size and segmentation method on trabecular bone microstructure measures in mice. *Bone Rep.* 2016 May;5:136-40. <https://doi.org/10.1016/j.bonr.2016.05.006>
7. Kim DG, Christopherson GT, Dong XN, Fyhrie DP, Yeni YN. The effect of microcomputed tomography scanning and reconstruction voxel size on the accuracy of stereological measurements in human cancellous bone. *Bone.* 2004 Dec;35(6):1375-82. <https://doi.org/10.1016/j.bone.2004.09.007>
8. Longo AB, Salmon PL, Ward WE. Comparison of ex vivo and in vivo micro-computed tomography of rat tibia at different scanning settings. *J Orthop Res.* 2017 Aug;35(8):1690-8. <https://doi.org/10.1002/jor.23435>
9. Chopra PM, Johnson M, Nagy TR, Lemons JE. Micro-computed tomographic analysis of bone healing subsequent to graft placement. *J Biomed Mater Res B Appl Biomater.* 2009 Feb;88(2):611-8. <https://doi.org/10.1002/jbm.b.31232>
10. Behrooz A, Kask P, Meganck J, Kempner J. Automated quantitative bone analysis in in vivo x-ray micro-computed tomography. *IEEE Trans Med Imaging.* 2017 Sep;36(9):1955-65. <https://doi.org/10.1109/TMI.2017.2712571>
11. Ding M, Odgaard A, Hvid I. Accuracy of cancellous bone volume fraction measured by micro-CT scanning. *J Biomech.* 1999 Mar;32(3):323-6. [https://doi.org/10.1016/S0021-9290\(98\)00176-6](https://doi.org/10.1016/S0021-9290(98)00176-6)
12. Dufresne T. Segmentation techniques for analysis of bone by three-dimensional computed tomographic imaging. *Technol Health Care.* 1998 Dec;6(5-6):351-9. <https://doi.org/10.3233/THC-1998-65-608>
13. Kuhn JL, Goldstein SA, Feldkamp LA, Goulet RW, Jesion G. Evaluation of a microcomputed tomography system to study trabecular bone structure. *J Orthop Res.* 1990 Nov;8(6):833-42. <https://doi.org/10.1002/jor.1100080608>
14. Elmoutaouakkil A, Peyrin F, Elkafi J, Laval-Jeantet AM. Segmentation of cancellous bone from high-resolution computed tomography images: influence on trabecular bone measurements. *IEEE Trans Med Imaging.* 2002 Apr;21(4):354-62. <https://doi.org/10.1109/TMI.2002.1000259>
15. Salarian A. Intraclass Correlation Coefficient (ICC): vesion 1.3.1.0. MathWorks. 2022 [cited 2016 Nov 15]. Available from: <https://uk.mathworks.com/matlabcentral/fileexchange/22099-intra-class-correlation-coefficient-icc>
16. Koo TK, Li MY. A guideline of selecting and reporting intraclass correlation coefficients for reliability research. *J Chiropr Med.* 2016 Jun;15(2):155-63. <https://doi.org/10.1016/j.jcm.2016.02.012>

17. Korfiatis VC, Tassani S, Matsopoulos GK. An Independent Active Contours Segmentation framework for bone micro-CT images. *Comput Biol Med.* 2017 Aug;87:358-70. <https://doi.org/10.1016/j.combiomed.2017.06.016>
18. Lublinsky S, Ozcivici E, Judex S. An automated algorithm to detect the trabecular-cortical bone interface in micro-computed tomographic images. *Calcif Tissue Int.* 2007 Oct;81(4):285-93. <https://doi.org/10.1007/s00223-007-9063-8>
19. Bissinger O, Götz C, Wolff KD, Hapfelmeier A, Prodingler PM, Tischer T. Fully automated segmentation of callus by micro-CT compared to biomechanics. *J Orthop Surg Res.* 2017 Jul;12(1):108. <https://doi.org/10.1186/s13018-017-0609-9>
20. Glatt V, Canalis E, Stadmeier L, Bouxsein ML. Age-related changes in trabecular architecture differ in female and male C57BL/6J mice. *J Bone Miner Res.* 2007 Aug;22(8):1197-207. <https://doi.org/10.1359/jbmr.070507>
21. Tjong W, Kazakia GJ, Burghardt AJ, Majumdar S. The effect of voxel size on high-resolution peripheral computed tomography measurements of trabecular and cortical bone microstructure. *Med Phys.* 2012 Apr;39(4):1893-903. <https://doi.org/10.1118/1.3689813>
22. Palacio-Mancheno PE, Larriera AI, Doty SB, Cardoso L, Fritton SP. 3D assessment of cortical bone porosity and tissue mineral density using high-resolution  $\mu$ CT: effects of resolution and threshold method. *J Bone Miner Res.* 2014 Jan;29(1):142-50. <https://doi.org/10.1002/jbmr.2012>
23. Waarsing JH, Day JS, Weinans H. An improved segmentation method for in vivo microCT imaging. *J Bone Miner Res.* 2004 Oct;19(10):1640-50. <https://doi.org/10.1359/JBMR.040705>
24. Gaêta-Araujo H, Oliveira-Santos N, Brasil DM, do Nascimento EH, Madlum DV, Haiter-Neto F, et al. Effect of micro-computed tomography reconstruction protocols on bone fractal dimension analysis. *Dentomaxillofac Radiol.* 2019 Dec;48(8):20190235. <https://doi.org/10.1259/dmfr.20190235>
25. Meganck JA, Kozloff KM, Thornton MM, Broski SM, Goldstein SA. Beam hardening artifacts in micro-computed tomography scanning can be reduced by X-ray beam filtration and the resulting images can be used to accurately measure BMD. *Bone.* 2009 Dec;45(6):1104-16. <https://doi.org/10.1016/j.bone.2009.07.078>